FIFTH AUSTRALASIAN CONFERENCE

on

HYDRAULICS AND FLUID MECHANICS

at

University of Canterbury, Christchurch, New Zealand

1974 December 9 to December 13

TAYLOR VORTEX BEHAVIOUR IN ANNULAR CLEARANCES OF LIMITED LENGTH

by

J. A. Cole

SUMMARY

Visual observations of the formation of Taylor vortices between concentric cylinders of radius ratio 0.7 and maximum length/radial clearance ratio 17 show that wide variations are possible in the number of vortex cells established for given operating conditions of speed, viscosity and annulus length. The significant factor is the route by which these operating conditions are set up. The effects of gradual acceleration from rest, impulsive starts from rest and annulus length variation while at speed are explored and indicate a wide range of possible stable vortex cell sizes, namely from 70 to 130% of the theoretical cell size. With slow acceleration from rest, the range is smaller, say 93 to 107% of the theoretical size, and it is suggested that the effect on the Taylor critical speed will be hardly detectable. Further experiments with cylinders of radius ratio 0.9 and maximum length/clearance ratio 45 confirm this, but demonstrate that the critical speed for the onset of the wave instability in Taylor vortices rises steeply as annulus length is reduced.

J.A. Cole, University of Western Australia

INTRODUCTION

The classical analysis by G.I. Taylor (1) of the stability of circumferential laminar flow between rotating cylinders deals with coaxial cylinders for which the length L is infinite and the radial clearance $R_2-R_1 = c$ is small. Although subsequent work has broadened the analysis to encompass finite clearances or eccentric cylinders, the assumption of infinite length remains, and most experimental workers aim at reproducing this condition as far as possible. In many situations of practical interest, short cylinders are involved, and as part of a continuing experimental investigation (2) of Taylor vortices in concentric and eccentric annular clearances the author has been studying vortex formation in a short annulus with $R_1/R_2 = 0.7$ and maximum $L/c = 17$.

The number of Taylor vortices possible in a given annulus length at a given supercritical rotational speed is surprisingly variable. For example, the author has photographed (slides to be shown at Conference) 7 different stable patterns of respectively 12, 13, 14, 15, 16, 17 and 18 cells for an annulus length $L = 15.2c$ using cylinders of radius ratio $R_1/R_2 = 0.728$ with the inner cylinder only rotating at 1.3 times the critical speed. A pattern of 15 cells gave sizes nearest to the expected value, the radial clearance c. However, starting the rotor from rest and gradually running up to speed yielded 14 cells, and the other patterns were obtained by varying the route by which the final operating conditions were achieved, e.g. by impulsive starts from rest to various speeds or by changes of annulus length once a particular vortex pattern had already been set up. This description of non-uniqueness and the implication of the significance of flow history are reminiscent of results reported by Coles (3) for the wavy (doubly periodic) mode of Taylor vortex flow with $R_1/R_2 = 0.88$ and by Snyder (4) for singly periodic Taylor vortex flow with $R_1/R_2 = 0.5$, both using fairly long annular clearances.

EXPERIMENTAL EQUIPMENT

The apparatus is a development of the vertical axis test rig already illustrated and described in reference (2). Now, the stationary outer cylinder is made of 19 mm thick Perspex of effective length 250 mm, with the bore turned and polished to give an internal diameter of 102.30 mm. The inner cylinder is one of a series of ground steel rotors, lengths 229 to 297 mm and diameters 15.24 to 99.73 mm. The test rotor is supported at the lower end in plain bearings with provision for offsetting the cylinder axes, and is driven via a worm gear box by a servo-controlled variable speed electric motor to give speeds from 0.1 to 100 rev/s. Speeds can be maintained constant to better than 0.1% for periods of several hours and can be measured to an accuracy better than 0.02% using a photocell and electronic counter. The lower end of the test annulus is a stationary solid surface. Usually, the oil depth sets the annulus test length and a free liquid surface exists at the upper end. To obtain symmetrical end conditions, an axially-adjustable stationary annular plate can be fitted to the stator. The test fluids are usually silicone oils, kinematic viscosity ν in the range 0.1 to 1 Stoke, with a small quantity of aluminium flakes (typical maximum dimension 0.01 mm) added to permit flow visualisation, and vortex cell sizes are measured in situ with a cathetometer. Flash photography has also been used, sometimes in conjunction with the thymol blue visualisation technique: a glycerol/water mixture then gives the required viscosity.

IMPULSIVE START TESTS

The variability of vortex cell numbers encountered in preliminary experiments and exemplified in the Introduction called for the adoption of a standardised operating procedure in an attempt to eliminate flow history effects. An impulsive start procedure was adopted at first : the annulus test length was set at zero speed, the rotor was accelerated to a pre-set operating speed by switching on the motor field control, and the vortex cell spacing was measured once the equilibrium pattern had been achieved. An operating angular velocity Ω about 13% above the calculated critical angular velocity Ω_c was chosen since this rapidly gave vortices sufficiently sharply defined for measurement with the cathetometer. With this standardised procedure, final vortex cell spacing was uniquely determined by the annulus length L and was uniform except for the single vortex cells occurring at the 'solid' and 'free' ends of the test annulus: these cells were respectively some 30% and 10% larger than the intervening cells.

During the acceleration period, vortex cells formed first at the two ends of the test annulus and succeeding cells rapidly spread axially inwards, with the initial spacing approximately 0.95c as determined from flash photographs. The rotor reached operating speed in about 2 seconds (the time for acceleration from 0.1 Ω to 0.9 Ω was 1.4 $\pm$ 3% s) and cells extended over the maximum full annulus length in about 8 s, adjusting to final size in a further 40 to 50 s. Snyder (4) quotes a spin-up time of $L/\sqrt{\nu\Omega}$, here 25 s, and reports a relaxation time of $L^2/6\nu$, here 156 s.

Measurements of the final equilibrium spacing of the individual vortex cells showed mean values V_m (excluding each end cell) ranging from about 0.8c to 1.2c, depending on the annulus length L. Sharply defined and repeatable discontinuous changes in vortex cell size occurred

periodically as annulus length was varied in small steps, consequent upon changes in the number n of cells accommodated. These changes, evident in Figure 1, presented an interesting visual appearance. At an annulus length slightly below one of these changeover lengths L^*, rotor acceleration from rest and the consequent axially inward spreading from the two ends of vortex cells of approximate size 0.95c led to the last-formed vortex pair at or near to the mid-point of the annulus having a size well below the standard 2c : this pair gradually diminished in size and finally disappeared as adjacent vortices adjusted to a larger size. The changeover length L^* was such that this central undersized pair was just able to survive. The size adjustment procedure now became slower, involving adjacent vortices diminishing in size as the central pair grew to equality. As annulus lengths were progressively increased above L^*, a stage was reached at which vortices retained their original size, so that further increase in annulus length again produced an extra under-sized pair, the situation already described.

Shorter annulus lengths required less time for the accomplishment of these changes in number of cells, and the details of the changes were then more difficult to follow. With a free liquid surface at the top of the test annulus, the adjustment procedure at the changeover length sometimes resulted in an odd number of cells (Figure 1 shows a maximum odd number of 5). All the top cells then readjusted, the odd cell having the same rotation as the bottom end cell. A single contra-rotating vortex pair occurred at annulus lengths as small as 1.8c (free surface) or 0.8c (solid upper surface).

Figure 2 shows the relationship between the number of cells accommodated n, and the annulus length, L. The changeover lengths L^* are linearly related to n except at very short lengths, and the reciprocal of the gradient is approximately 0.96 c. Further investigation showed that this gradient depends on the value of the final operating speed Ω used in the standardised impulsive start procedure, and the reciprocal gradient tends to the value c as the speed is reduced to the Taylor critical value Ω_c , i.e. changeover lengths L^* are increased by about 0.3% per 1% reduction in speed.

Measurements of flash photographs of the transient stages of vortex pattern development following an impulsive start from rest are hampered by the diffuse boundaries of newly formed cells. The general trend is clear: initial cell sizes (with one exception) diminish with increase of final operating speed, the rate being -0.2 to -0.5% per 1% rise in speed above critical, with the free surface end cell showing the most change. Limiting initial sizes as $\Omega \to \Omega_c$ are 1.3c for the bottom end cell, 1.2c for the top end cell and 1.0c for the intervening cells. The initial stages of the last-formed vortex pair were particularly elusive, but the limiting single cell size seems to be 0.5c $\pm$ 10% at Ω_c and this size increases at perhaps 1% per 1% rise in operating speed above critical. Increase of operating speed well above Ω_c introduces new complications: the survival of the last-formed vortex pair now depends on resistance to the onset of a transient wave-like instability of seemingly random occurrence and changeover lengths are less repeatable. The wavy vortex mode was not encountered here as a steady state condition.

GRADUAL START RESULTS

When flow patterns at full annulus depth were observed during gradual increase of speed from rest, a single cell, initially of vague and shadowy form and of size roughly 0.5c, first appeared at the lower (solid surface) end of the annulus at speeds as low as about 0.4 Ω_c. A second cell, nearer in size to c, made a shadowy appearance at about 0.7 Ω_c , and both had fairly clearly defined boundaries at about 0.8 Ω_c , with helical motion of the aluminium marker particles now clearly evident in the bottom cell. Further increase of speed soon led to the appearance, again initially in shadowy form, of cells at the top end of the annulus and of further cells at the lower end, but a complete array of vortices did not appear until the calculated critical speed Ω_c was attained, with slow equalization there. Gradual increase of speed above the critical had only a minor effect on the vortex pattern established at the critical speed, apart from intensifying the helical motion of marker particles in each cell and sharpening cell boundaries. Cathetometer measurements showed that the bottom cell decreased very slightly in size, about -0.01% per 1% speed increase above Ω_c, the top free surface cell increased in size at an even lower rate, and the intervening cells maintained their size constant within the accuracy of the measurements for speeds up to 1.5 Ω_c. These last observations are broadly in line with those obtained by Burkhalter and Koschmieder (5) using a far wider range of speeds.

Small step-wise variations of annulus length yielded well-defined changeover lengths at which the number of cells accommodated changed suddenly. At the maximum annulus length tested, rotor acceleration was found to have a small effect. Thus the changeover lengths for 14 to 16 cells occurred at lengths 214.1, 214.4 and 215.0 $\pm$ 0.05 mm for accelerations 0.027, 0.009 and 0.003 rad/s^2 respectively. No variation was detectable for the changeover from 6 to 8 cells, and most of the results presented here were taken at the two higher accelerations. Figure 3 shows the relationship between number of cells and annulus length : the reciprocal gradient is 1.00 c. Thus

FIGURE 1 Variation of vortex cell sizes V with annulus length L: impulsive starts.

$R_1/R_2 = 0.713$ $\Omega/\Omega_c = 1.13$

(a) Asymmetric end conditions

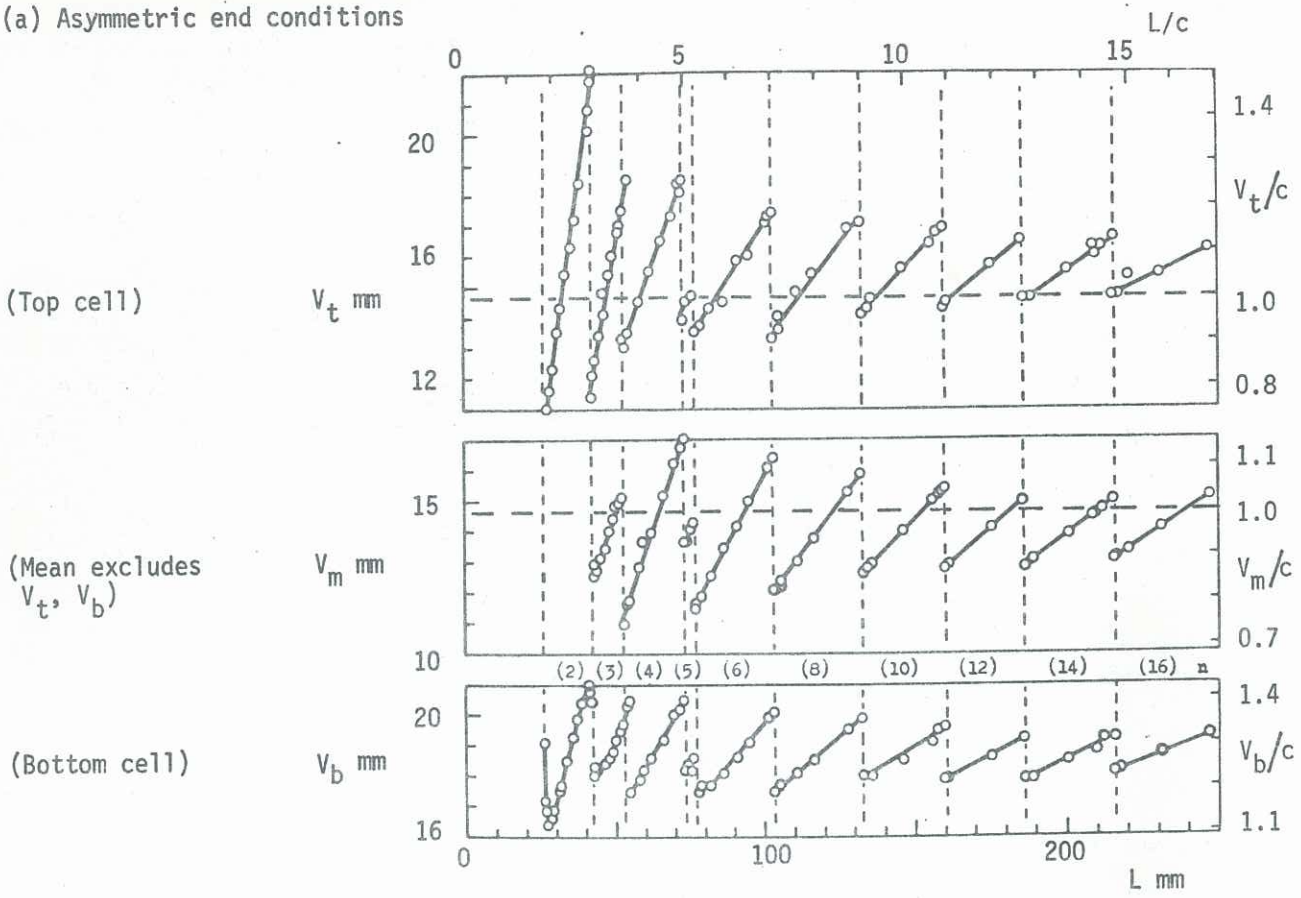

(b) Symmetric end conditions

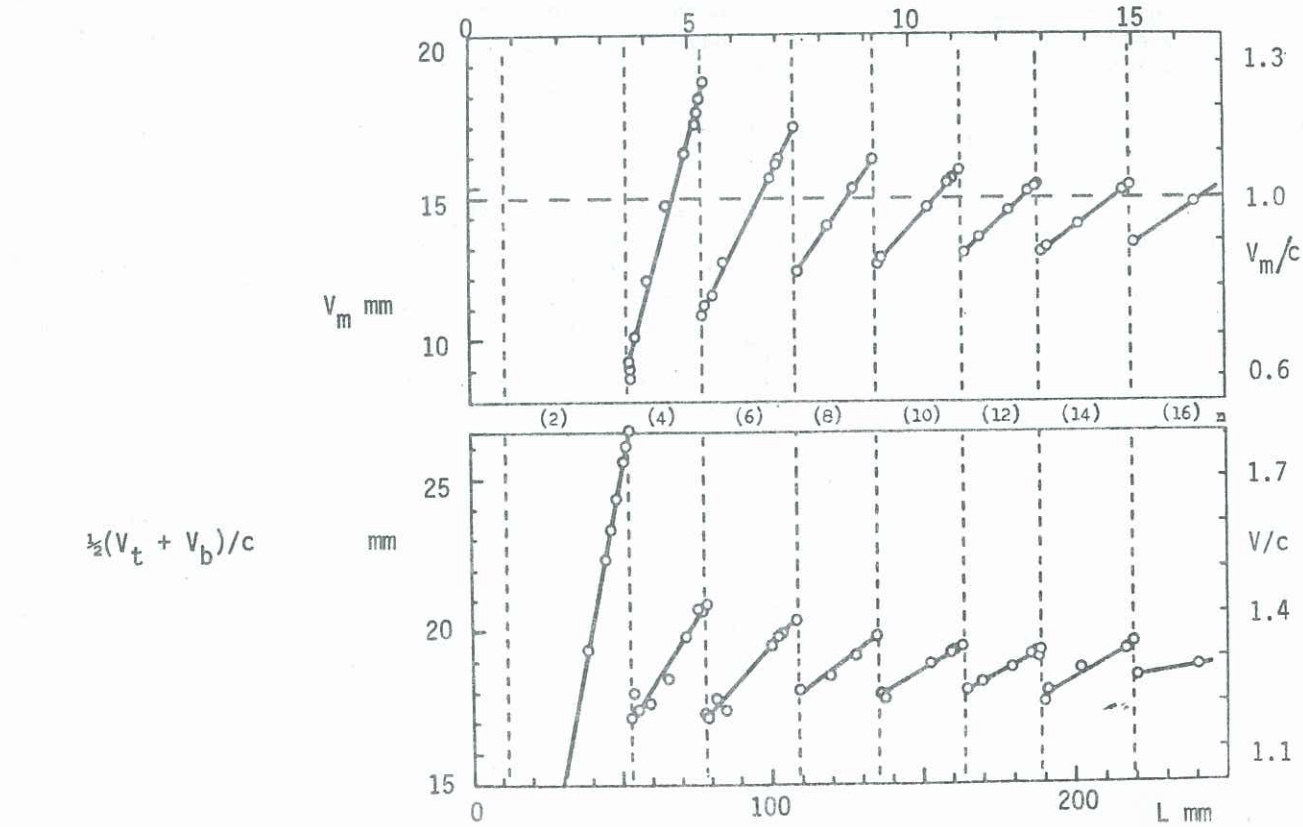

the results for a gradual start are in fair agreement with the impulsive start results of Figure 2 and reduction of the speed for impulsive start would improve the agreement, as already indicated.

EXPANSION AND COMPRESSION OF VORTEX CELLS

When fluid was allowed to flow slowly into or out of the base of the test annulus while the rotor was running at a given supercritical speed, the vortex cells were observed to expand or contract as the annulus length changed, and periodically the number of cells altered suddenly. The number of cells accommodated and the changeover lengths were found to vary with the rate of inflow or outflow and with the operating speed. Consistent results were obtained when flow rates were small and carefully controlled and when operating speeds were sufficiently in excess of the critical speed to give reasonably rapid adjustment of cell size. Very high flow rates merely caused the vortex pattern to translate bodily with the rise or fall of the free liquid surface.

Figure 4 shows changeover lengths observed for stepped inflow and outflow at rotor speeds 1.13 Ω_c and 1.3 Ω_c. Very small flow increments (equivalent to level changes of about 0.4 mm in 15 seconds or an axial flow Reynolds Number of the order of 0.01) followed by a zero flow period of 2 minutes were employed near changeover points. Vortex systems were obtained similar to those already described, except that a 5 cell system was not obtained at the higher speed. Again, the changeover points for even numbers of cells are collinear, indicating regular periodicity. At the lower speed, the reciprocal gradients are 1.20 c for inflow and 0.82 c for outflow (average 1.01 c) and at the higher speed, the reciprocal gradients are 1.27 c for inflow and 0.76 c for outflow (average 1.02 c). A similar graph was obtained at a rotor speed 1.02 Ω_c , but slow cell adjustment made changeover lengths more difficult to determine satisfactorily. The reciprocal gradient turned out to be close to c, as the foregoing results would suggest.

Rapid inflows to the top of the test annulus via the rotor gave an additional effect : at certain flow rates sequences 4, 5, 6, 7, ... and 5, 7, 9, ... cells were achieved at about 1.1 Ω_c . The cells in an existing vortex pattern could also be expanded or compressed by carefully moving upwards or downwards a non-rotating annular plate sliding inside the stator, but this procedure has so far proved to be less convenient than the fluid inflow or outflow technique just described.

RANGE OF STABLE VORTEX SIZES

Figure 5 shows mean vortex cell sizes V_m (end cells excluded) measured in the steady state at a speed 1.13 Ω_c for a range of annulus lengths (free upper surface) with $R_1/R_2 = 0.728$. The various vortex patterns were obtained by appropriate combinations of gradual or impulsive starts with vortex compression or expansion. The speed chosen gave sharply defined cell boundaries well-suited to cathetometer measurement and also gave reasonably rapid cell size adjustment with change of conditions. As remarked earlier, change of operating speed has virtually no effect on steady state cell sizes in a given vortex pattern. On the other hand, the vortex expansion and compression results show that higher operating speeds would give a greater range of cell sizes than is seen in Figure 5.

The number of different vortex patterns possible at a given annulus length at 1.13 Ω_c is given by the number of intersections of the cell size lines with the appropriate annulus length ordinate in Figure 5, and evidently this number increases with annulus length. Increase of speed further increases the number, while decrease of speed produces the opposite effect. As speed is reduced to Ω_c , a given vortex pattern slowly reverts to the unique pattern obtained in gradual start tests. Thus the 7 different patterns instanced in the Introduction to illustrate the variety of vortex patterns which may be encountered at the same operating conditions all revert to a pattern of 14 cells when the speed is reduced from 1.3 Ω_c to Ω_c.

The question arises as to whether limiting sizes of stable vortex cells can be determined. Figure 6 shows the effect of operating speed on maximum and minimum mean sizes for a 14 or 10 cell pattern, sizes being adjusted by the cell expansion and compression technique. At high speeds, limiting sizes seemed to become quasi-stable, and at low speeds, size adjustment was very slow, but results were reasonably repeatable and general trends are clear: stable cells can vary in size from 0.7c to 1.3c in this instance, compared with the theoretical size c. This range far exceeds the range of cell sizes, namely 0.93c to 1.07c, occurring with a gradual start from rest for annulus lengths producing 14 to 16 cells. On the other hand, photographs of the fleeting appearances of the last-formed vortex pair in impulsive starts from rest suggest a transient minimum cell size as low as 0.5c.

In the conventional stability analysis, the theoretical vortex cell size c follows from the assumption that the critical speed corresponds to the minimum in the stability plot relating Reynolds Number and disturbance wave number. Figure 7 shows the computed relationship for

FIGURE 2 Impulsive starts $R_1/R_2 = 0.713$

FIGURE 3 Gradual starts, $R_1/R_2 = 0.728$

(N.B. zigzag lines show no. of cells n at any length L; thicker straight lines join changeover points L*)

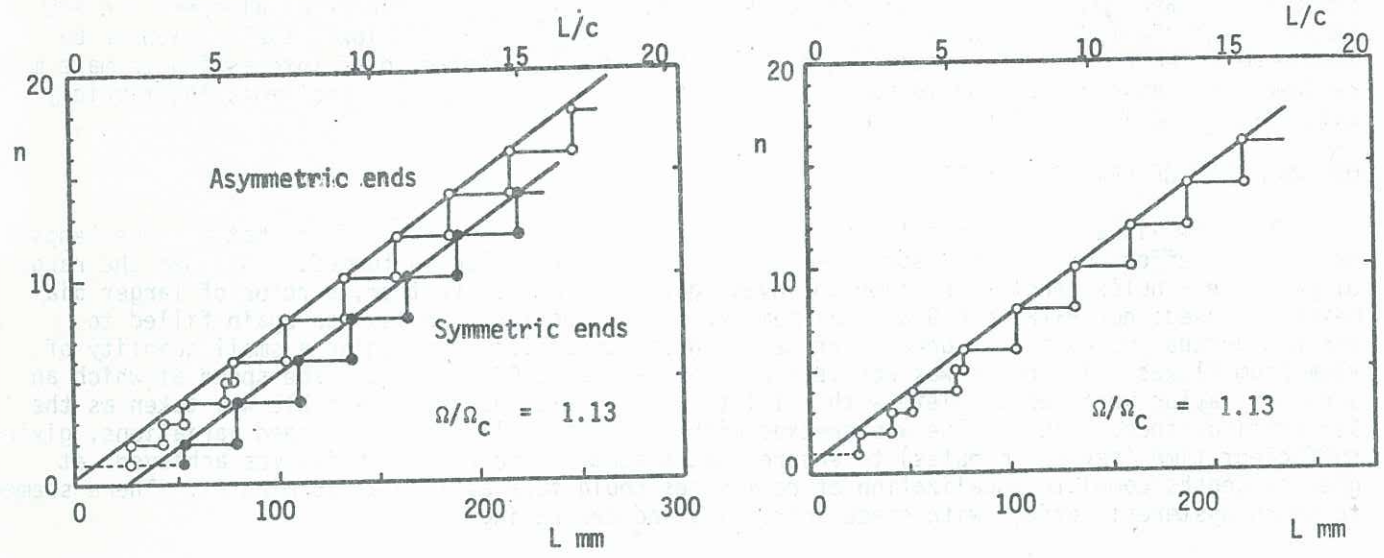

FIGURES 4 Vortex cell expansion & compression by fluid inflow & outflow, $R_1/R_2 = 0.728$

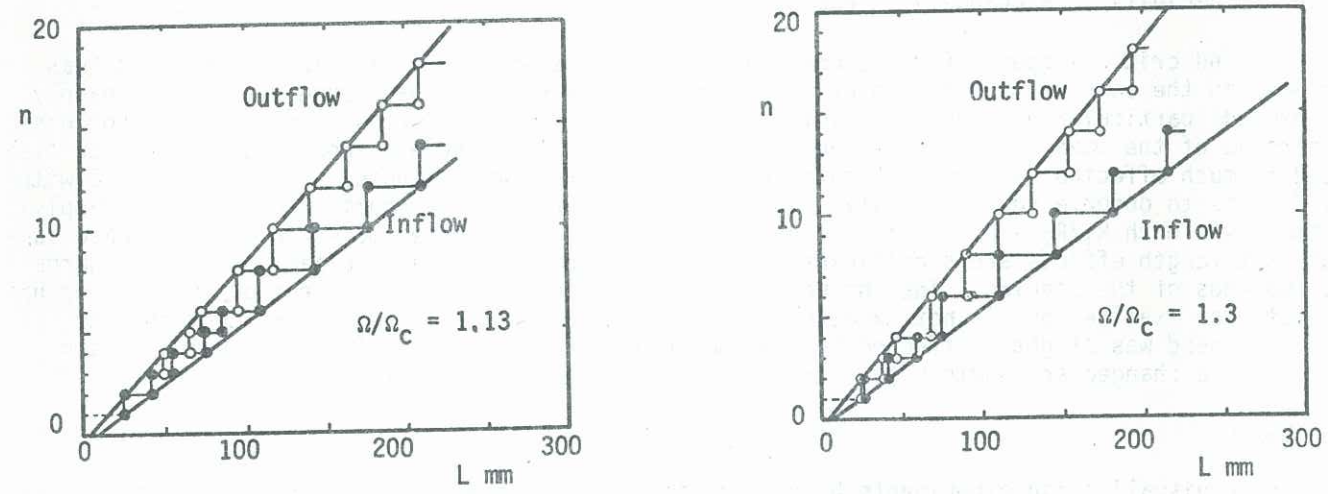

FIGURE 5 Vortex cell mean sizes (end cells excluded), $R_1/R_2 = 0.728$

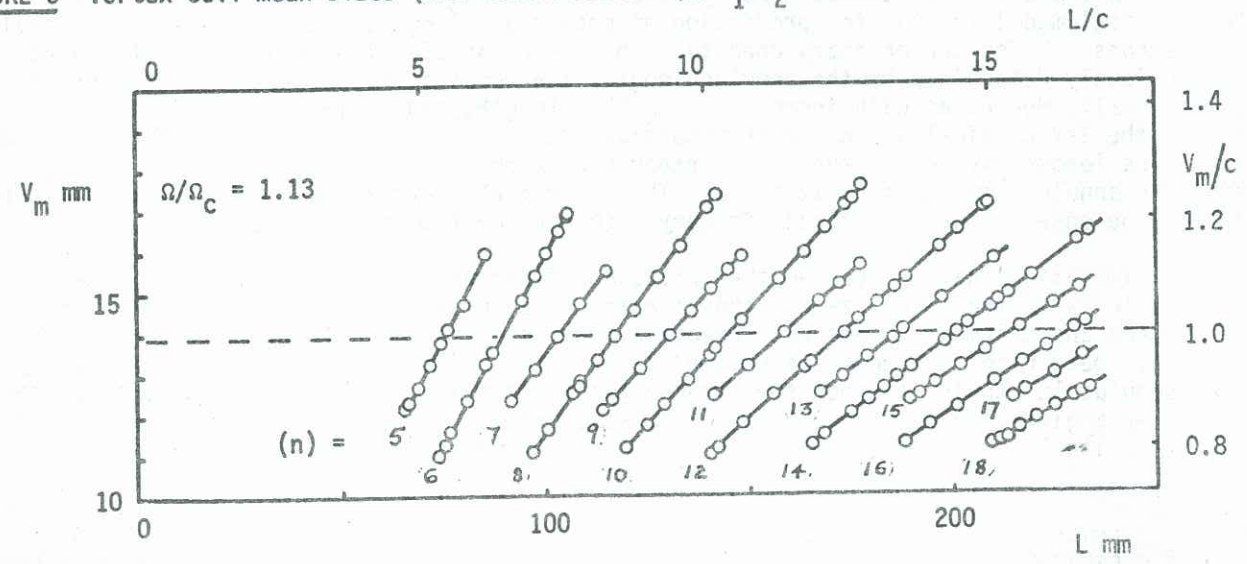

R_1/R_2 = 0.729 using a linearised analysis for infinitely long concentric cylinders of finite clearance. The minimum Reynolds Number is 306.0 at a wave number of 11.6 which yields a cell size of 1.00c. The gradual start cell size range 1.07c to 0.93c given above corresponds to Reynolds Numbers from 306.9 to 307.2 in Figure 7 i.e. to + 0.29% and + 0.39% changes in critical speed. For a longer annulus, the cell size range is smaller and the changes in critical speed are lower still. Such small deviations would not be very reliably detected by flow visualization or by torque measurement with the present equipment. Nevertheless, it would be interesting to make more refined observations and also to have a stability analysis developed to deal more legitimately with finite annulus lengths.

OBSERVATIONS OF CRITICAL SPEEDS

The flow visualization results presented so far for R_1/R_2 = 0.7 suggest that annulus length may have an effect on critical speeds as well as on numbers of cells formed. To widen the range of possible annulus lengths in order to investigate this effect further, a rotor of larger diameter was used: now R_1/R_2 = 0.9 and maximum L/c = 45. The test annulus was again filled to various depths, using a free upper surface, with silicone fluid containing a small quantity of aluminium flakes. The rotor was accelerated from rest at 0.007 rad/s and the speed at which an array of Taylor vortices complete with all inter-cell divisions became visible was taken as the 1st critical speed. This value was checked with adjacent small step-wise speed variations, giving sufficient time (several minutes) to ensure that a state of near-equilibrium was achieved; at greater depths complete equalization of cell sizes could take as long as 15 minutes. There seemed to be no hysteresis effect with speed increasing and decreasing.

It was found, as shown in Figure 8, that the 1st critical speed was substantially independent of annulus length but showed a slight decrease at small lengths. However the criterion for the completeness of the vortex pattern became less clear-cut when the fluid depth was low, particularly if in the vicinity of a changeover length L^*.

The 2nd critical speed, for the onset of the wave instability in the Taylor vortices, was examined in the same way and the point of appearance of wavy cells was found to be very sharply delineated, particularly at greater fluid depths. At the critical speed, the appearance or disappearance of the wave instability required several minutes. Figure 8 shows that the 2nd critical speed is much affected by annulus length, rising steeply at small lengths. This is in line with the failure to observe persistent wavy vortices with the relatively short annulus lengths applying to the tests with R_1/R_2 = 0.7. Visual observation of the wavy vortex mode would in any case suggest that length effects are significant: the amplitude of the waves is clearly smaller towards the two ends of the annulus. The influence of a solid boundary at the top end of the annulus has not yet been examined but is not expected to be marked. There were indications that the 2nd critical speed was slightly affected by the number of cells present at a given annulus length (i.e. near a changeover length L^*) but this requires further investigation.

CONCLUSION

These visualization experiments have emphasised the variability in the number of Taylor vortex cells which may be set up in short annular clearances and the consequent range of possible cell sizes. A comparison of the data for gradual and impulsive starts suggests that the author's simple empirical model (2) for the prediction of changeover lengths could be extended to deal with both situations. Under the ordinary conditions of a slow acceleration from rest, the number of cells is uniquely determined by the annulus length: the variability in cell size is then comparatively small, decreases with increase in annulus length, and would not be expected to affect noticeably the 1st critical speed. With impulsive starts from rest, the number of cells in a given annulus length may be greater, and further variation in cell size may be effected by altering the annulus length while at speed. The experiments have shown that the 2nd critical speed, for the onset of wavy vortices, is very much dependent on annulus length.

Space limitations have prevented the inclusion of torque measurements made separately from but in parallel with the visualization experiments. Discontinuities in torque/speed graphs show up the 1st and 2nd critical speeds well except at very small annulus lengths and confirm that the 2nd critical speed rises as length is reduced. The 1st critical speed becomes progressively less clear as annulus length is reduced: the customary discontinuity in the torque/speed graph becomes rounded. For a given length, the torque is the same whether the operating speed is achieved by a gradual or an impulsive start even though the numbers of vortex cells established may differ in the two cases. It has therefore been very surprising to find that the torque does change significantly if for a given annulus length and operating speed the number of cells is changed by vortex expansion or compression and this is now being investigated. Space limitations also prevent inclusion of experiments with eccentric cylinders, but no particularly unusual results have been encountered here.

FIGURE 6 Limiting sizes of stable vortex cells
$R_1/R_2 = 0.728$

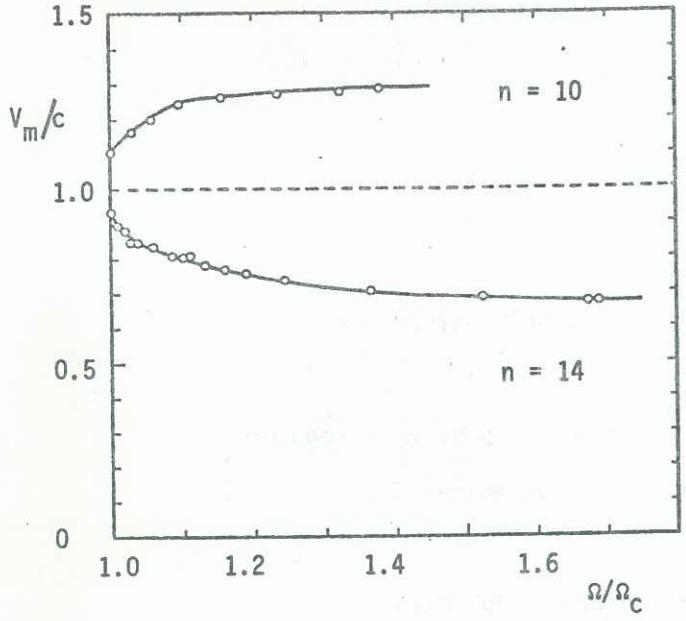

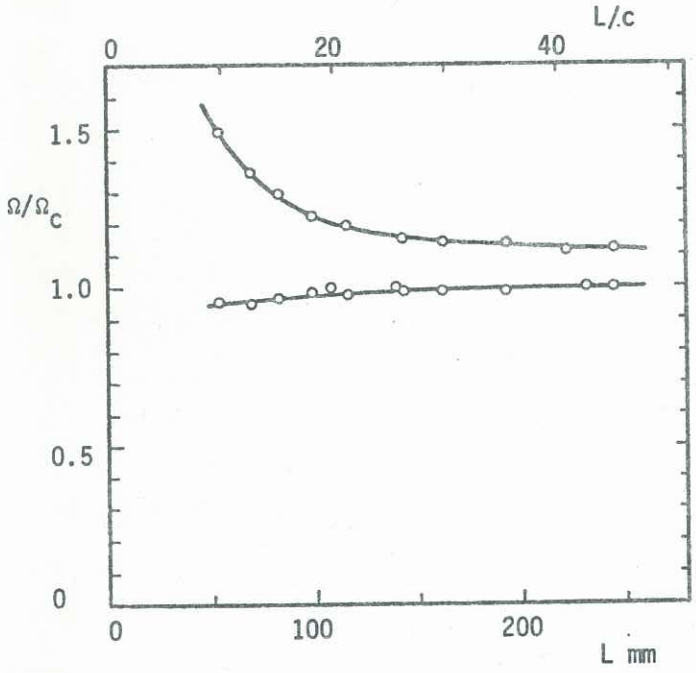

FIGURE 7 Theoretical stability diagram
$R_1/R_2 = 0.729$ (1st critical)

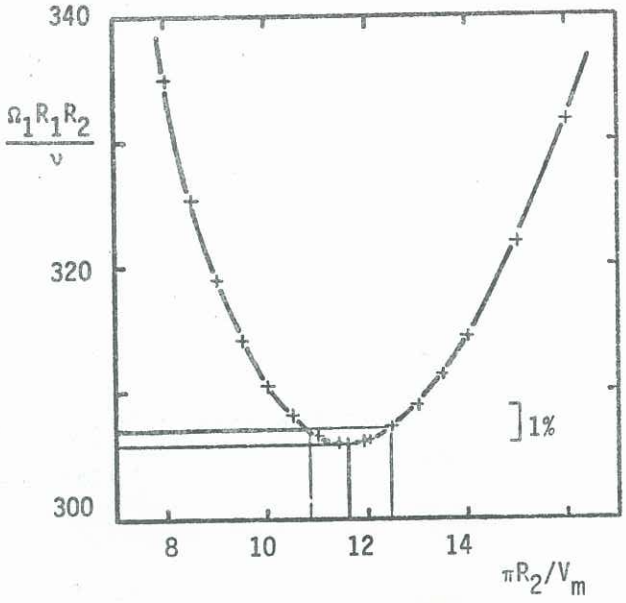

FIGURE 8 Critical speeds and annulus length

$R_1/R_2 = 0.894$

Lower curve: 1st critical (Ω_c)

Upper curve: 2nd critical (wavy)

ACKNOWLEDGEMENTS

The author's experimental work has been helped by equipment grants from the University of W.A. and the Australian Research Grants Committee, by equipment construction by members of the Mechanical Engineering Department Workshop and by the sympathetic encouragement of Professor David Allen-Williams. The computations involved in preparing Figure 7 were carried out by Allan D. Thomas.

REFERENCES

1. Taylor, G.I. 1923 Phil. Trans. Roy. Soc., A, 223, 289-343.
2. Cole, J.A. 1971 Proc. 4th Aust. Conf. Hydraulics & Fluid Mech, 27-34.
3. Coles, D. 1965 J. Fluid Mech., 21, 385-425.
4. Snyder, H.A. 1969 J. Fluid Mech., 35, 273-298.
5. Burkhalter, J.E. & Koschmieder, E.L. 1973 J. Fluid Mech., 58, 547-560.
6. Cole, J.A. 1974 J. Fluids Eng. 96, 69-72.